Nanoscale Res Lett (2010) 5:1124–1127
DOI 10.1007/s11671-010-9612-3

NANO EXPRESS

Fabrication and Optical Behaviors of Core–Shell ZnS Nanostructures

Zai-Xing Yang · Wei Zhong · Yu Deng · Chaktong Au · You-Wei Du

Received: 1 April 2010 / Accepted: 12 April 2010 / Published online: 24 April 2010

Abstract Novel core–shell nanostructures comprised of cubic sphalerite and hexagonal wurtzite ZnS have been synthesized at 150°C by a simple hydrothermal method. The results of HR-TEM and SAED investigation reveal that the cores of hexagonal wurtzite ZnS (ca. 200 nm in average diameter) are encapsulated by a shell of cubic sphalerite ZnS. The FE-SEM image of the nanomaterials shows a surface tightly packed with nanoparticles (<10 nm in size). The optical properties of the fabricated material have been studied in terms of ultraviolet–visible absorption and photoluminescence. Furthermore, a possible mechanism for the fabrication of the core–shell nanostructures has been presented.

Keywords ZnS · Core–shell nanostructures · Optical properties

Introduction

As an important member of II–VI group semiconductors of wide band gap, zinc sulfide (ZnS) has been extensively investigated. The material is utilized in a wide range of applications, e.g. photocatalysts, photoconductors, optical sensors, optical coatings, electrooptic modulators, field effect transistors, electroluminescent materials, solid-state solar window layers, light-emitting materials, etc. [1]. ZnS has two known crystallographic structures, viz. hexagonal wurtzite and cubic sphalerite, which show band gaps of 3.77 eV [2] and 3.72 eV [3], respectively at room temperature (RT). The hexagonal phase is thermodynamically metastable and is only stable at temperatures higher than 1,020°C [4] whereas the cubic phase is thermodynamically stable at RT. However, based on results of molecular dynamics simulations as well as thermodynamic analysis, Zhang et al. reported that nanoparticles of wurtzite ZnS is thermodynamically more stable than those of sphalerite ZnS in vacuum [5]. In the last decade, many reports on the production of ZnS are for sphalerite ZnS rather than wurtzite ZnS, plausibly due to the metastable nature of the latter. Nevertheless, it has been reported that hexagonal ZnS nanocrystals can be produced at a relatively low temperature through solvothermal reactions [6, 7]. It is known that ZnS can transform spontaneously from hexagonal to cubic structure upon contact with some organic molecules (e.g. pentafluorothiophenol, thiophenol, 1-decanethiol, 1-hexanethiol, benzoic acid and cyanoacetic acid) at ambient temperature [8]. In terms of optical properties, wurtzite ZnS is generally considered more desirable than sphalerite ZnS. It is hence meaningful to find ways that wurtzite ZnS can be protected from entities that would induce phase transformation.

The fabrication of complex three-dimensional (3D) architectures of ZnS (assembled by nanostructured ZnS as building blocks) with controlled morphology, orientation and dimensionality has attracted much attention in the past decade because the structures may provide opportunities to exploit novel properties such as high surface area and surface permeability [9, 10]. ZnS assemblies having superior nature with 3D structures such as solid and hollow nanospheres [11], hierarchical structures [12] and

Z.-X. Yang · W. Zhong (✉) · Y. Deng · Y.-W. Du
Nanjing National Laboratory of Microstructures and Department of Physics, Nanjing University, 210093 Nanjing, People's Republic of China
e-mail: wzhong@mail.nju.edu.cn

C. Au
Chemistry Department, Hong Kong Baptist University, Hong Kong, People's Republic of China

submicrotubes [13] have been reported. Recently, ZnS nanostructures with different morphologies and sizes were fabricated through low cost, simple and efficient hydrothermal method. For example, quantum-sized ZnS nanocrystals with quasi-spherical and rod shapes were synthesized using alkylamine [14], bundles of wurtzite ZnS nanowires were synthesized using hydrazine hydrate [15], two-dimensional wurtzite ZnS nanostructures was fabricated from ethylenediamine [16], spherical nanostructures comprised of ZnS nanocrystals were obtained in aqueous solutions [6], and ZnS nanoparticles and nanorods were fabricated with controlled crystallinity through a solvothermal approach involving the change of solvent used for synthesis [1].

In this paper, we report the synthesis (at 150°C) of a novel 3D ZnS core–shell nanostructure via a simple one-step hydrothermal procedure. The metastable wurtzite ZnS is encapsulated by a shell of sphalerite ZnS so that the wurtzite ZnS core can be protected from the outside environment. The results show that the approach is efficient and the outcome highly reproducible. To the best of our knowledge, the fabrication of such a core–shell nanostructure through hydrothermal reaction has never been reported before.

Experimental Section

All the reagents used for the synthesis of the core–shell material were of analytical grade (purchased from Nanjing Chemical Industrial Co.) and used without further purification. First, 14.87 g zinc nitrate [$Zn(NO_3)_2{\cdot}6H_2O$] and 40.0 g NaOH were dissolved in deionized water to form a 100.0 ml solution. Then 3.0 ml of the solution was mixed with 5.0 ml of deionized water and 25.0 ml of absolute ethanol (C_2H_5OH), followed by the addition of 5.0 ml of aqueous ammonia (25%). Before being transferred into a Teflon-lined autoclave, an appropriate amount of sublimed sulfur powder (in Zn:S molar ratio of 3:1, 1:1 and 1:3) was added and the mixture was vigorously stirred for 30 min. Subsequently, the autoclave with its content was kept in an oven at 150°C for 24 h. At the end of the hydrothermal treatment, the as-obtained solid material was separated using a centrifuge, and thoroughly washed with absolute ethanol and deionized water (3 cycles).

The as-obtained materials were examined on an X-ray powder diffractometer (XRD) at room temperature (RT) for phase identification using Cu Kα radiation (Model D/Max-RA, Rigaku). The morphology of samples was examined over a high-resolution transmission electron microscope (HR-TEM, JEOL-2010, operated at an accelerating voltage of 200 kV) and a field emission scanning electron microscopy (FE-SEM, FEI Sirion 200, operated at an accelerating voltage of 5 kV). The optical properties of the materials were investigated for ultraviolet–visible (UV–vis) absorption (Cary, USA) and photoluminescence (PL, excitation source: He-Cd laser, 325 nm) at RT.

Results and Discussion

As shown in Fig. 1, the X-ray diffraction (XRD) results of the solid products show ZnS of hexagonal wurtzite (JCPDS No. 75-1547) as well as cubic sphalerite (JCPDS No. 05-0566) phases. The strong and shape peaks assignable to wurtzite ZnS indicate good crystallization and grain formation. In contrast, the broad peaks of sphalerite ZnS show the size effect of nanocrystallites. Using the Scherrer formula with deal consideration to the FWHM (full width at half maximum) of peaks, the average grain size of sphalerite ZnS is estimated to be around 10 nm. Hence, despite bulk wurtzite ZnS is metastable below 1,020°C, stable wurtzite ZnS can be fabricated under hydrothermal conditions with temperature as low as 150°C. The results of XRD also indicate that the crystal structure of the final products is strongly related to the Zn:S molar ratio. The product obtained at Zn:S of 3:1 is a mixture of sphalerite and wurtzite ZnS, whereas at Zn:S of 1:3, the product is mainly sphalerite ZnS.

The high-resolution transmission electron microscopy image of the product synthesized at Zn:S of 3:1 shows core/shell quasi-spheres with external diameters of around 500 nm (Fig. 2). The cores (with size of about 200 nm) seem to be in the course of evolution from irregular to hexagonal shape. The shell is composed of tiny particles with size of several nanometers. The insets of Fig. 2 show the selected-area electron diffraction (SAED) patterns

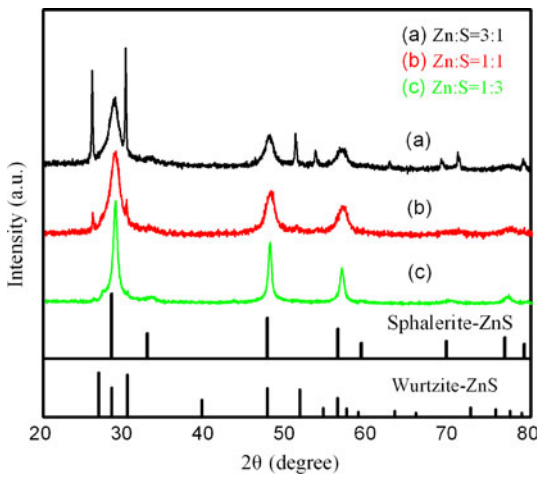

Fig. 1 XRD patterns of the products obtained at different Zn:S molar ratios. The XRD pattern of standard wurtzite and sphalerite structures of ZnS are also shown

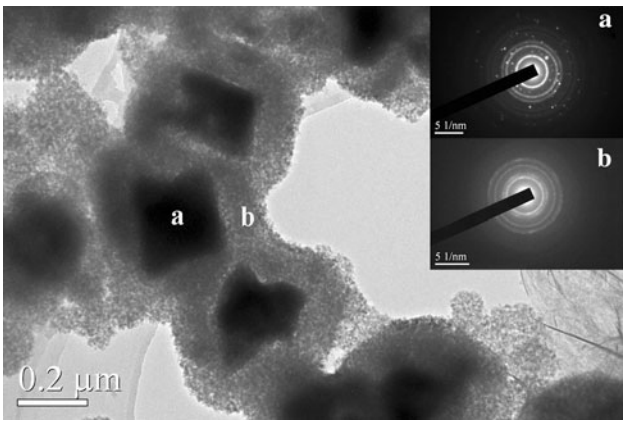

Fig. 2 HR-TEM image of the product obtained at Zn:S of 3:1. The *insets* are the SAED patterns recorded on region of **a** both core and shell and **b** shell only of the nanostructures

recorded at (a) region of both core and shell and (b) region of shell only. It is clear that the former suggests the presence of sphalerite and wurtzite phases, while the latter the sole presence of sphalerite phase, which is consistent with the XRD results.

Field emission scanning electron microscopy and energy dispersion spectroscopy (EDS) were employed to characterize the product fabricated with Zn:S = 3:1. Figure 3a shows that the core–shell nanostructures are oval and the surface is tightly packed with nanoparticles. According to the EDS data (Fig. 3b), the obtained product is comprised of Zn and S elements with Zn:S molar ratio close to 1:1 (i.e. the stoichiometry of ZnS).

Although the exact mechanism for the formation of the core–shell nanostructures is unclear, one can make certain deduction based on known information. First, we know that without the introduction of sulfur powder but following the same procedure, wurtzite ZnO is the final product [17]. Also, in an alkali solution and under high pressure (condition of hydrothermal treatment in an autoclave), sulfur is transformed to S^{2-} and SO_3^{2-} through a disproportionation reaction:

$$3S + 6OH^- \rightarrow 2S^{2-} + SO_3^{2-} + 3H_2O$$

It is possible that cubic and hexagonal ZnS are formed through two different ways: (1) hexagonal wurtzite ZnS is formed from hexagonal wurtzite ZnO via S^{2-} substitution of O^{2-} under the conditions of hydrothermal treatment; in other words, ZnO acts as a template for the formation of wurtzite ZnS [18]; (2) cubic sphalerite ZnS nanoparticles are formed through a facile reaction between S^{2-} and Zn^{2+}. At Zn:S of 1:3, path (2) dominates.

We measured the room-temperature ultraviolet–visible (UV–vis) absorption and photoluminescence of the obtained materials fabricated at Zn:S = 3:1 (core–shell nanostructured ZnS) and Zn:S = 1:3 (cubic sphalerite ZnS). As shown in the UV–vis absorption spectra (Fig. 4a), the two materials exhibit excitonic absorption at ~291 nm (with a tail at 301 nm) and 310 nm. Compared to the corresponding peak of bulk ZnS (onset is at 340 nm), there is a modest blue shift possibly due to quantum-size effects. The long absorption tail (between 400–800 nm) in the case of cubic sphalerite ZnS (Zn:S = 1:3) was due to scattering by the crystals [19]. In addition, with the rise of Zn:S ratio from 1:3 to 3:1, a red shift from 291 nm (or 301 nm) to 310 nm was observed. From the TEM images, one can see that the average size of the wurtzite ZnS cores is the biggest when Zn:S ratio is 3:1. We hence attribute the red shift to the increase in average radius of the nanocrystallites. In Fig. 4b, the PL spectra of core–shell ZnS (obtained at Zn:S = 3:1) and cubic sphalerite ZnS (obtained at Zn:S = 1:3) exhibit strong emissions at 545 nm and 524 nm, respectively, along with an identical weak shoulder at about 617 nm. The low-energy luminescence at 617 nm could be due to defects other than Schottky vacancies inside the nanostructures. The nature of visible emission at 524 nm is not clear. Liu et al. related the green emission observed over sphalerite ZnS to some self-activated centers, probably vacancy states or interstitial states of the peculiar structure [20]. Such understanding could be helpful to explain the 545-nm emission observed in the present study. Furthermore, compared to the PL spectrum

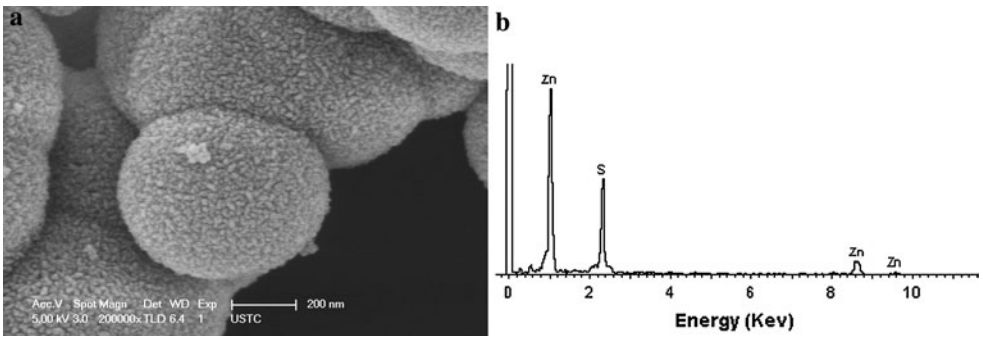

Fig. 3 **a** FE-SEM image and **b** EDS spectrum of the product obtained at Zn:S of 3:1

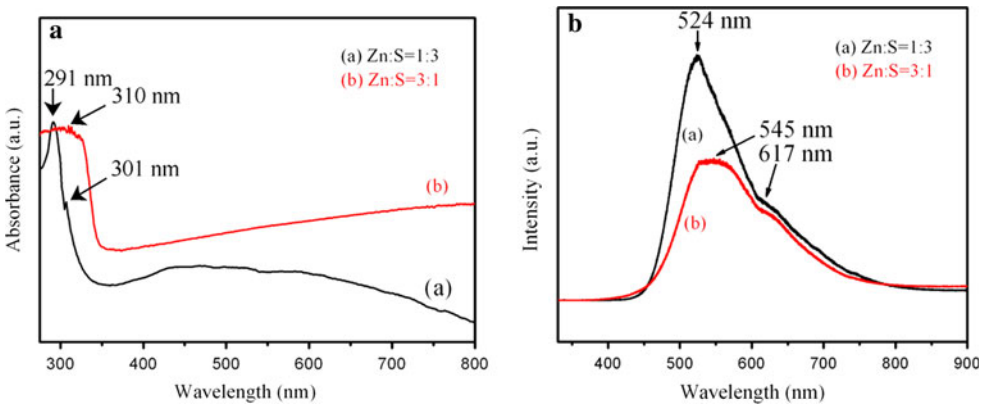

Fig. 4 **a** UV–vis absorption and **b** PL spectrum of the product obtained at Zn:S of 3:1 (core–shell nanostructured ZnS) and 1:3 (cubic sphalerite ZnS)

of sphalerite ZnS, the strong emission center of core–shell ZnS exhibits a red shift (~21 nm). The results demonstrate that the excitonic absorption and PL emission can be tuned by simply controlling the Zn:S ratio.

Conclusions

In summary, novel core–shell material comprised of cubic sphalerite (shell) and hexagonal wurtzite (core) ZnS were synthesized at 150°C using zinc nitrate and sulfur as source materials via a simple hydrothermal method. The generation of the core–shell nanostructures might involve two steps: (1) the formation of wurtzite ZnS using ZnO (hexagonal) as template, and (2) the formation of a shell of sphalerite ZnS nanoparticles via a facile reaction between S^{2-} and Zn^{2+}. By simply controlling the Zn:S ratio, one can tune the optical properties of the material such as excitonic absorption and PL emission.

Acknowledgments We would like to acknowledge the Foundation of National Laboratory of Solid State Microstructures, Nanjing University (Grant No. 2010ZZ18), the National High Technology Research and Development Program of China (Grant No. 2007AA021805), and the National Key Project for Basic Research (Grant No. 2005CB623605), People's Republic of China for financial support.

References

1. S. Biswas, S. Kar, Nanotechnology **19**, 045710 (2008)
2. H.C. Ong, R.P.H. Chang, Appl. Phys. Lett. **79**, 3612 (2001)
3. T.K. Tran, W. Park, W. Tong, M.M. Kyi, B.K. Wagner, C.J. Summers, J. Appl. Phys. **81**, 2803 (1997)
4. L. Yin, Y. Bando, Nat. Mater. **4**, 883 (2005)
5. H.Z. Zhang, F. Huang, B. Gilbert, J.F. Banfield, J. Phys. Chem. B **107**, 13051 (2003)
6. H. Tong, Y.-J. Zhu, L.-X. Yang, L. Li, L. Zhang, J. Chang, L.-Q. An, S.-W. Wang, J. Phys. Chem. C **111**, 3893 (2007)
7. W.Y. Zhao, Y. Zhang, H. Zhu, G.C. Hadjipianayis, J.Q. Xiao, J. Am. Chem. Soc. **126**, 6874 (2004)
8. K. Murakoshi, H. Hosokawa, N. Tanaka, M. Saito, Y. Wada, T. Sakata, H. Mori, S. Yanagida, Chem. Commun. **321** (1998)
9. G.M. Whitesides, B. Grzybowski, Science **295**, 2418 (2002)
10. J.M. Lehn, Science **295**, 2400 (2002)
11. F. Gu, C.Z. Li, S.F. Wang, M.K. Lu, Langmuir **22**, 1329 (2006)
12. Q. Zhao, Y. Xie, Z. Zhang, X. Bai, Cryst. Growth Des. **7**, 153 (2007)
13. G.Z. Shen, Y. Bando, D. Golberg, Appl. Phys. Lett. **88**, 123107 (2006)
14. H.Y. Jung, J. Jin, M.P. Hyun, B. Sung-Il, W.K. Young, C.K. Sung, T. Hyeon, J. Am. Chem. Soc. **127**, 5662 (2005)
15. L. Chai, D. Jin, S. Xiong, H. Li, Y. Zhu, Y. Qian, J. Phys. Chem. C **111**, 12658 (2007)
16. G.T. Zhou, X. Wang, J.C. Yu, Cryst. Growth Des. **5**, 1761 (2005)
17. B. Liu, H.C. Zeng, J. Am. Chem. Soc. **125**, 4430 (2003)
18. D. Farah, E.S. Raymond, J. Am. Chem. Soc. **131**, 424 (2009)
19. J. Nanda, S. Sapra, D.D. Sarma, Chem. Mater. **12**, 1018 (2000)
20. X.Z. Liu, J.H. Cui, L.P. Zhang, W.C. Yu, F. Guo, Y.T. Qian, Mater. Lett. **60**, 2465 (2006)